The American Journal of Pathology, Vol. 182, No. 2, February 2013

The American Journal of
PATHOLOGY
ajp.amjpathol.org

METABOLIC, ENDOCRINE, AND GENITOURINARY PATHOBIOLOGY

New Therapeutic Approach to Suppress Castration-Resistant Prostate Cancer Using ASC-J9 via Targeting Androgen Receptor in Selective Prostate Cells

Kuo-Pao Lai, Chiung-Kuei Huang, Yu-Jia Chang, Chin-Ying Chung, Shinichi Yamashita, Lei Li, Soo Ok Lee, Shuyuan Yeh, and Chawnshang Chang

From the Departments of Pathology, Urology, and Radiation Oncology, the George Whipple Laboratory for Cancer Research, and the Wilmot Cancer Center, University of Rochester Medical Center, Rochester, New York

Accepted for publication October 31, 2012.

Address correspondence to Chawnshang Chang, Ph.D., Departments of Pathology and Urology, University of Rochester Medical Center, 601 Elmwood Ave., Box 626, Rochester, NY 14642. E-mail: chang@urmc.rochester.edu.

Using androgen receptor (AR) knockout mice to determine AR functions in selective prostate cancer (PCa) cells, we determined that AR might play differential roles in various cell types, either to promote or suppress PCa development/progression. These observations partially explain the failure of current androgen deprivation therapy (ADT) to reduce/prevent androgen binding to AR in every cell. Herein, we identified the AR degradation enhancer ASC-J9, which selectively degrades AR protein via interruption of the AR-AR selective coregulator interaction. Such selective interruption could, therefore, suppress AR-mediated PCa growth in the androgen-sensitive stage before ADT and in the castration-resistant stage after ADT. Mechanistic dissection suggested that ASC-J9 could activate the proteasome-dependent pathway to promote AR degradation through the enhanced association of AR-Mdm2 complex. The consequences of ASC-J9-promoted AR degradation included reduced androgen binding to AR, AR N-C terminal interaction, and AR nuclear translocation. Such inhibitory regulation could then result in suppression of AR transactivation and AR-mediated cell growth in eight different mouse models, including intact or castrated nude mice xenografted with androgen-sensitive LNCaP cells or androgen-insensitive C81 cells and castrated nude mice xenografted with castration-resistant C4-2 and CWR22Rv1 cells, and TRAMP and *Pten*$^{+/-}$ mice. These results demonstrate that ASC-J9 could serve as an AR degradation enhancer that effectively suppresses PCa development/progression in the androgen-sensitive and castration-resistant stages. *(Am J Pathol 2013, 182: 460–473; http://dx.doi.org/10.1016/j.ajpath.2012.10.029)*

Androgen/androgen receptor (AR) signaling plays essential roles in prostate cancer (PCa) progression and results in castration resistance.[1–4] Currently, most, if not all, androgen deprivation therapy (ADT) targets androgens via surgical and/or medical castration to reduce/prevent androgen binding to AR.[5] However, few, if any, of these ADTs with various antiandrogens, including the recently developed enzalutamide,[6] have the capacity to eliminate all PCa cells in the later castration-resistant stage. Therefore, degradation of AR during/after ADT can be considered to have clinical benefits for patients with advanced PCa with substantial AR.[6] These conclusions suggest that identifying a novel compound(s) that could degrade/diminish AR protein in the castration-resistant stage, unlike currently used antiandrogens, may yield better therapeutic efficacies to battle PCa in the castration-resistant stage.

Early studies via isolation of three PCa primary cells (PCa1, PCa2, and PCa3) from the same patient found that androgen/AR signaling could function differentially to either suppress or promote PCa growth.[7] Using the cre-loxP strategy in mice to selectively knockout *AR* in various PCa

Supported by NIH grants (CA127300, CA122840, and CA156700) and the George Whipple Professorship Endowment.

K.-P.L. and C.-K.H. contributed equally to this work.

Disclosure: ASC-J9 was patented by the University of Rochester, the University of North Carolina, and AndroScience Corp. and then was licensed to AndroScience Corp. The University of Rochester and C.C. own royalties and equity in AndroScience Corp.

http://dx.doi.org/10.1016/j.ajpath.2012.10.029

cells, Niu and colleagues[3,4,8] observed that the loss of AR in cytokeratin 5/cytokeratin 8−positive basal intermediate epithelial cells led to increased PCa metastasis, yet loss of AR in cytokeratin 8−positive luminal epithelial cells resulted in suppressed PCa progression with increased cell apoptosis. In contrast, loss of AR in stromal fibroblasts and smooth muscle cells resulted in suppression of prostate/PCa growth.[9,10] These results conclude that AR can either promote or suppress PCa progression in different types of PCa cells.

Because only one *AR* gene has been identified,[11] we hypothesized that these differential AR roles in various PCa cells in the same patient could be due to the existence of different AR-AR coregulator complexes. This hypothesis led us to screen the AR degradation enhancer 5-hydroxy-1,7-bis(3,4-dimethoxyphenyl)-1,4,6-heptatrien-3-one (ASC-J9) from natural products and their derivatives by selectively interrupting the interaction between AR and selective AR coregulators, such as AR−AR-associated protein (ARA) 70 and AR-ARA55, which are expressed mainly in luminal epithelial cells and stromal cells, respectively, in which AR may function with positive roles to either maintain cell survival or promote cell proliferation. Results from four different human PCa cell lines and eight different *in vivo* mouse models concluded that ASC-J9 could function as a promising AR degradation enhancer to suppress PCa progression before and after castration resistance with few adverse effects.

Materials and Methods

Mice, Cells, Reagents, and Human Prostate Specimens

The *Pten*$^{+/-}$ mouse (B6/129 background) was originally obtained from the National Cancer Institute (Bethesda, MD) and was backcrossed into C57BL/6 background for five or six generations. The protocols of *Pten* genotyping were used according to the previous report.[12] TRAMP mice in FVB or C57BL/6 background were purchased from The Jackson Laboratory (Bar Harbor, ME). The tumor chunks from C57BL/6 TRAMP mice were used for SCID mouse implantation, and FVB/C57BL/6 TRAMP mice were used for ASC-J9 injection experiments. Animal study protocols were approved by the University of Rochester Committee on Animal Resources, and the mice were kept in a specific pathogen−free environment.

PCa cell lines LNCaP, C4-2, C81, CWR22Rv1, and LAPC4 were cultured in RPMI medium supplemented with 10% fetal bovine serum (FBS), 100 U/mL of penicillin/streptomycin, and 2 mmol/L L-glutamine (Life Technologies, Carlsbad, CA). Prostate stromal cells WPMY-1 and COS-1 were cultured in Dulbecco's modified Eagle's medium supplemented with 10% FBS, 100 U/mL of penicillin/streptomycin, and 2 mmol/L L-glutamine (Life Technologies). 5α-Dihydrotestosterone (DHT; Sigma-Aldrich, St. Louis, MO) was dissolved in 100% ethanol and was stored at −20°C for up to 1 month. Bicalutamide (Casodex) and hydroxyflutamide (HF) were purchased from Toronto Research Chemicals (Toronto, Ontario, Canada) and were dissolved in dimethyl sulfoxide (DMSO). Enzalutamide (formerly known as MDV3100; Selleck Chemicals, Houston, TX), MG-132 (Sigma-Aldrich), and LY294002 (Calbiochem, Millipore, Billerica, MA) were dissolved in DMSO. The antibodies for AR (N-20), ARA55, ARA70, estrogen receptor (ER) α, glucocorticoid receptor (GR), peroxisome proliferator-activated receptor (PPAR) α, PPARγ, retinoic acid receptor α (RARα), murine double minute protein 2 (Mdm2), and glyceraldehyde-3-phosphate dehydrogenase (GAPDH) were purchased from Santa Cruz Biotechnology (Santa Cruz, CA). The ERβ antibody was obtained from Genoptix (Carlsbad, CA). The antibodies for SRC-1, pAkt at Ser 473, total Akt, and pMdm2 at S166 were purchased from Cell Signaling Technology Inc. (Danvers, MA), and Ki-67 was from Novocastra Laboratories Ltd. (Newcastle on Tyne, UK). The plasmids pDNA3-HA-Ub, dominant-negative Akt (myr-Akt K179M, T308A, and S473A), and mutant Mdm2 (S166/186A) were obtained from Addgene (Cambridge, MA).

ASC-J9 was a gift from AndroScience Corp. (San Diego, CA) and was generated as described previously.[13,14] ASC-J9 [dissolved in *N,N*-dimethylacetamide and diluted with Kolliphor EL (formerly known as Cremophor EL; Sigma-Aldrich) and 0.9% normal saline] was i.p. injected into mice at a dose of 50, 75, or 100 mg/kg as described until the end of each study. Control mice received *N,N*-dimethylacetamide, Kolliphor EL, and 0.9% normal saline diluent only. For the *in vitro* study, ASC-J9 was dissolved in DMSO at 10 mmol/L and was stored at −20°C.

Paired human primary prostate tissues were collected from the same patients before ADT and after the development of castration-resistant PCa at Tohoku University Hospital (Sendai, Japan), Miyagi Cancer Center (Natori, Japan), and Chang Gung Memorial Hospital (Taipei, Taiwan). The study was approved by the ethics committees of the three institutions.

ASC-J9 Characterization

For the study of AR-ARA55 and AR-ARA70 interactions, WPMY-1 and LNCaP cells were treated with vehicle, bicalutamide, or 5 μmol/L ASC-J9 and then were analyzed using the co-immunoprecipitation (Co-IP) assay. Before drug treatment, 5 μmol/L MG-132 was added to the culture medium for 30 minutes to prevent AR protein degradation.[15] For the AR-Mdm2 interaction study, we used LNCaP cells and followed the same protocol as described previously. For the mammalian two-hybrid assay to determine the AR-AR coregulator interaction, COS-1 cells were seeded and transfected with pGal4-RE-Luc reporter plasmid, pCMX-Gal4-AR-LBD (AR ligand binding domain), pCMX-VP16-ARA70, or pCMX-VP16-ARA55 plasmids, and we followed the protocol as described previously.[16] The AR transactivation activity was monitored using ARE_4-luciferase or MMTV-luciferase as previously described.[14] For the AR protein degradation study, LAPC4, LNCaP, C4-2, and

C2R22Rv1 cells were cultured in RPMI medium plus 10% charcoal-dextran–stripped (CDS) FBS for 2 days. The next day, cells were treated with vehicle or 1 nmol/L DHT and 5, 7.5, or 10 μmol/L ASC-J9 in 10% CDS-FBS RPMI medium. The treatments with the antiandrogens enzalutamide, bicalutamide, and HF were used as controls. After 24 hours of treatment, the cell lysates were harvested and subjected to AR and GAPDH Western blot analysis. The stabilities of AR, GR, ERα, ERβ, PPARα, PPARγ, and RARα in response to 5 μmol/L ASC-J9 were tested in LNCaP cells (AR and RARα), PC3 cells (GR, PPARα, and PPARγ), and T47D cells (ERα and ERβ) by using Western blot analysis.

Ubiquitination Assay

CWR22Rv1 cells were transiently transfected with pCDNA3-HA-Ub (Addgene) by Lipofectamine 2000 (Invitrogen, Carlsbad, CA) for 6 to 8 hours. After transfection, the medium was replaced with 10% CDS-FBS RPMI medium for 24 hours. Then, the cells were treated with ethanol, 1 nmol/L DHT, or 1 nmol/L DHT/10 μmol/L ASC-J9 for another 24 hours. The cell extracts were harvested and subjected to Co-IP assays. We used HA antibody (Genoptix) to pull down the ubiquitinated AR and AR antibody (N-20; Santa Cruz Biotechnology) for the immunoblotting assay.

Competitive Binding Studies

Aliquots of the lysates were incubated with 5 nmol/L [^{3}H] R1881 (90 Ci/mmol) in the absence or presence of unlabeled corticosteroids (DHT, HF, and ASC-J9, 1×10^{-10} to 1×10^{-1} mol/L, in a final reaction volume of 100 μL). Binding of ^{3}H-labeled androgen was measured using the hydroxyapatite filter method. The inhibitory concentration of 50% was determined by measuring the amount of DHT required to inhibit the binding of 5 nmol/L [^{3}H] R1881 to AR by 50% and was determined from the competitive binding curves. The inhibitory concentration of 50% of each compound was calculated according to the plots of concentration versus percentage of binding. The experiments were repeated three times to ensure the binding specificity. The variations of duplicated assays were within 10% of the average (Supplemental Table S1).

Immunofluorescence Staining

LNCaP cells were cultured in 2-well Chamber slides (Nalge Nunc International Corp., Rochester, NY) and treated with vehicle, 1 nmol/L DHT, or 1 nmol/L DHT/5 μmol/L ASC-J9 in 10% CDS-FBS RPMI medium with the addition of 50 μmol/L cycloheximide (Sigma-Aldrich). Cells were then fixed and stained with AR antibody, followed by fluorescein isothiocyanate–conjugated secondary antibody (Vector Laboratories, Burlingame, CA). The slides were mounted in fluorescent mounting medium containing DAPI (Vector Laboratories). Fluorescent staining was observed using an Olympus fluorescent microscope (IX71; Olympus America Inc., Center Valley, PA).

Chromatin Immunoprecipitation

C4-2 cells were cultured in 10% CDS-FBS RPMI medium for 2 days and were treated with vehicle, 1 nmol/L DHT, 5 μmol/L ASC-J9, or 1 nmol/L DHT/5 μmol/L ASC-J9 for 4 hours. The cells were subjected to standard chromatin immunoprecipitation assay as described previously.[13] The eluted products were detected by using quantitative real-time PCR, and the AR-binding DNA was pulled down by using AR antibody (C-19; Santa Cruz Biotechnology). The input control was used to normalize each treated group, and IgG control served as negative control.

Cell Growth Assay

C4-2, C81, CWR22Rv1, and LNCaP cells were seeded in 24-well plates at a density of 2000 cells per well in RPMI medium containing 10% CDS-FBS for 24 hours. The cells were treated with vehicle, 1 nmol/L/10 nmol/L DHT, 5 μmol/L HF, 5 μmol/L bicalutamide, or 5 μmol/L ASC-J9. The medium was replenished every other day, and cell growth was determined using MTT assay. Serum-free medium containing MTT (0.5 mg/mL; Sigma-Aldrich) was added to each well. After 2 hours of incubation at 37°C, the medium was removed and DMSO was added to solubilize the formazan product, and the absorbance was recorded using an enzyme-linked immunosorbent assay reader.

RNA Extraction, RT-PCR, Quantitative Real-Time PCR, and Pathway-Focused Superarray Analysis

Total RNAs were prepared from cells using TRIzol reagent (Invitrogen) according to the manufacturer's instructions. cDNA synthesis was performed by using RT-PCR with SuperScript RNase H-Reverse Transcriptase (Invitrogen). Expression levels of AR-regulated genes were determined by quantitative real-time PCR using iCycler real-time PCR amplifier (Bio-Rad Laboratories, Hercules, CA). The relative copy numbers of GAPDH or β-actin were quantified and used for normalization. The $\Delta\Delta C_T$ method was used to calculate relative differential expression between the control and experimental groups. For the Cancer PathwayFinder Superarray analysis (PAMM-033; SABioscience, Invitrogen), >80 primers corresponding to several category-related genes (cell cycle control and DNA damage repair, apoptosis and cell senescence, signal transduction molecules and transcription factors, adhesion, angiogenesis, and invasion/metastasis) were precoated on 96-well plates from SABioscience (Invitrogen). The standard real-time PCR analysis was used, and the analysis was conducted using

website-based software RT2 Profiler PCR Array Data Analysis version 3.5 (Qiagen Inc., Valencia, CA).

Animals Studies

Xenografted Mouse Models

For orthotopic xenografts, C81, C4-2, CWR22Rv1, and LNCaP cells were harvested, washed with PBS, and resuspended in Matrigel (a 1:1 mixture of culture medium and Matrigel) (BD Biosciences, San Jose, CA). The C81 (2×10^6 per site), LNCaP (2×10^6 per site), C4-2 (5×10^5 per site), or CWR22Rv1 (5×10^5 per site) cells were then injected orthotopically into two anterior prostate lobes of nude mice. For the s.c. injection study, LNCaP or C81 cells (2×10^6 per site) were injected into two flanks of the 5- to 6-week-old male nude mice.

The effects of ASC-J9 on xenografted tumor growth under the castration condition. The orthotopic implantation and surgical castration were performed simultaneously. After 2 to 3 weeks of tumor development, vehicle or 75 mg/kg of ASC-J9 was given by i.p. injection every other day for 2 weeks ($N = 5$ to 6 mice per group).

The effects of ASC-J9 on PCa development/progression in intact nude mice. For PCa early development, treatment with ASC-J9 started when LNCaP cells were injected for xenograft in the flanks. Thirty-six mice were separated into three groups: vehicle control, 50 mg/kg of ASC-J9, and implanted HF pellet. Tumor size was monitored twice a week and was scored as positive (end point) when the size reached 40 mm^3. For PCa development/progression, ASC-J9 treatment was started after the tumor developed (2 to 3 weeks after xenografts). Mice were randomly separated into three groups (12 mice and 24 tumors per group: vehicle control, 50 mg/kg of ASC-J9, and 100 mg/kg of ASC-J9). The treatment schedule was twice per week, and the flank tumor size was measured twice per week using calipers. The following formula was used to estimate tumor weight: tumor size (mm^3) = tumor length (mm) $\times$ [tumor width (mm)]^2 $\times 0.5$.

TRAMP and *Pten*$^{+/-}$ Mouse Models

For the TRAMP mouse model, C57BL/6/FVB TRAMP mice were treated with 75 mg/kg of ASC-J9 or vehicle control through i.p. injections every day at 8 weeks old ($N = 6$ mice per group). Starting at 10 weeks old, the mice were examined weekly until they were 23 to 24 weeks old. The mice were euthanized with carbon dioxide, and necropsy was performed to confirm the presence and origin of the tumor. For the *Pten*$^{+/-}$ mouse model, 6-month-old C57BL/6 *Pten*$^{+/-}$ mice were treated with vehicle control or 100 mg/kg of ASC-J9 three times per week for 2 months. At 8 months of age, the prostate tissues were harvested and subjected to histologic characterization.

TRAMP Mouse Tumor Chunk Implantation

The prostate tumors were harvested from 33- to 34-week-old C57BL/6 TRAMP mice and cut into 0.2-cm tissue chunks. The tissue chunks were implanted into SCID mice s.c. or as subrenal capsule implants to examine ASC-J9 therapeutic effects *in vivo*.

For s.c. implantation, the prostate tumor chunks were s.c. implanted into SCID mice. After 2 weeks of tumor growth, vehicle control or 100 mg/kg of ASC-J9 was injected into SCID mice three times per week. After 4 weeks of treatment, the tumors were harvested and the tumor weights determined. For subrenal capsule implantation, the prostate tumor chunks were implanted into SCID mouse subrenal capsules. After 2 weeks of tumor growth, vehicle control or 100 mg/kg of ASC-J9 was injected into mice three times per week. After 4 weeks of treatment, the tumors grown under the subrenal capsule were harvested and the tumor weights determined.

Histologic Characterization

The xenografted prostate tumor tissues were harvested and immediately immersed into 10% neutral buffered formalin for overnight incubation. The tissues were embedded as paraffin blocks and sectioned at 5 μm for H&E staining and immunohistochemical staining using specified antibodies. Tissue slides were prepared, and sodium citrate (pH 6.0) was applied for antigen retrieval. The 5% bovine serum albumin and 5% nonfat milk in 0.1% phosphate-buffered saline/Tween buffer was used for blocking at room temperature for 1 hour. The primary antibodies against AR (N-20; Santa Cruz Biotechnology), Ki-67 (Novocastra Laboratories Ltd.), and SV40-T antigen (Santa Cruz Biotechnology) were used for hybridization at 4°C overnight, and secondary antibody with conjugated horseradish peroxidase was applied for staining and substrate development. The BrdU staining (Invitrogen) and terminal deoxynucleotidyl transferase-mediated dUTP nick-end labeling (TUNEL) assay (Calbiochem) were performed according to the manufacturer's instructions.

Statistical Analysis

The experiments were repeated a minimum of three times, and the data are presented as mean ± SD or mean ± SEM. Statistical significance was determined using the *t*-test (two-tailed) comparison between two groups of data sets. One-way analysis of variance was used to compare more than two groups. $P < 0.05$, $P < 0.01$, and $P < 0.001$ were considered statistically significant depending on the experiment.

Results

ASC-J9 Interrupts the Interaction between AR and AR Coregulators ARA55 and ARA70 in Prostate Stromal WPMY-1 and Luminal Epithelial LNCaP Cells

To selectively target AR in PCa stromal and/or luminal epithelial cells in PCa progression, we started with a comprehensive

tissue survey to examine the expressions of previously identified AR coregulators[17] and, consistent with previous reports, identified ARA55 and ARA70 expression, mainly in stromal and luminal epithelial cells, respectively.[16,18] We then screened natural products and their derivatives to determine which ones could interrupt the interaction between AR-ARA55 in prostate stromal WPMY-1 cells and/or AR-ARA70 in luminal epithelial LNCaP cells. We found that ASC-J9, but not the currently used antiandrogens, such as bicalutamide, could promote the dissociation of AR-ARA55 complex in WPMY-1 cells by using the Co-IP assay and the mammalian two-hybrid assay (Figure 1A). A similar observation was seen in AR-ARA70 complex in LNCaP cells with ASC-J9 treatment (Figure 1B).

Such interrupted association of AR-ARA55 in WPMY-1 cells and of AR-ARA70 in LNCaP cells resulted in suppression of stromal AR−targeted gene keratinocyte growth factor and epithelial AR−targeted gene prostate specific antigen (PSA) expression (Figure 1C). We found that ASC-J9 had less effect in interrupting the interaction between AR and AR coregulator SRC-1 in LNCaP cells (Supplemental Figure S1), suggesting that ASC-J9 could differentially interrupt the interactions between AR and selective AR coregulators.

Together, the results from Figure 1, A−C, demonstrate that interruption of the AR-ARA55 interaction in WPMY-1 stromal cells and the AR-ARA70 interaction in LNCaP luminal epithelial cells suppressed AR transcriptional activity, which was further confirmed using the $(ARE)_4$-luciferase assay (Figure 1D). We found that ASC-J9 could also suppress HF-, bicalutamide-, and 17β-estradiol−induced AR transactivation in the presence of ARA70, which might contribute to the androgen-independent AR-mediated PCa progression in the castration-resistant stage (Figure 1, E−G).[19]

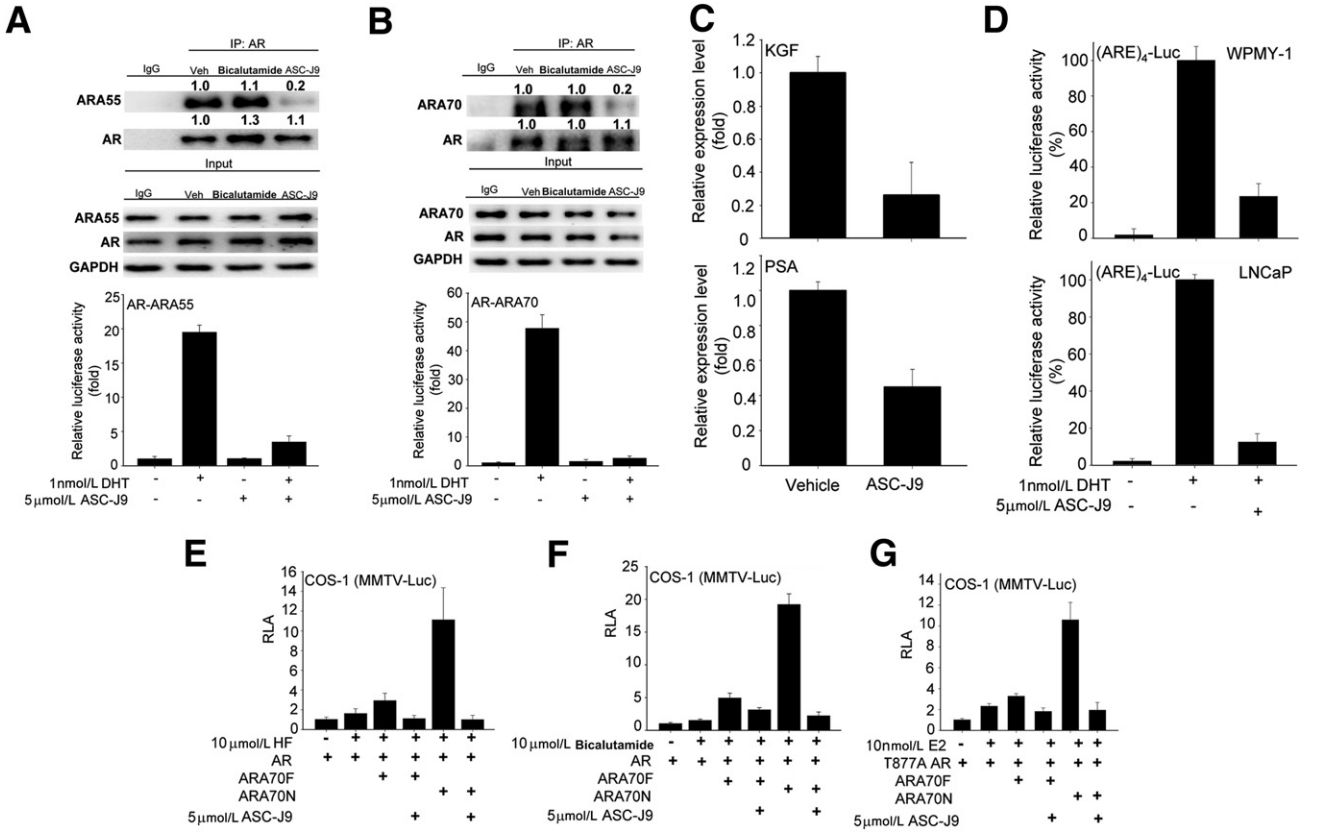

Figure 1 ASC-J9 selectively promotes AR degradation via interrupting the interaction between AR and AR coregulators. **A:** ASC-J9 disrupted the interaction between AR and ARA55 in WPMY-1 cells. **Top and middle panels:** Co-IP assay of the AR-ARA55 complex in WPMY-1 cells examined by immunoblotting assay. The 5 μmol/L proteasome inhibitor MG-132 was added for 30 minutes before adding the vehicle (Veh), 5 μmol/L bicalutamide, or 5 μmol/L ASC-J9 to prevent protein degradation. The quantitation data of Co-IP are presented as fold increase compared with the Veh group by densitometric analysis of bands. The input loading controls show similar amounts. **Bottom panel:** The mammalian two-hybrid assay was used to demonstrate that 5 μmol/L ASC-J9 can suppress the interaction between AR and ARA55. **B:** ASC-J9, 5 μmol/L, dissociated the binding of AR and ARA70 in LNCaP cells. **Top and middle panels:** Co-IP of AR-ARA70 complex in LNCaP cells, with or without ASC-J9 treatment, and determined by immunoblotting assay. MG-132 at 5 μmol/L was added before treatment. The quantitation of Co-IP results are presented as fold increase compared with the Veh group. **Bottom panel:** ASC-J9 also showed the inhibitory effects on the interaction between AR-ARA70 by mammalian two-hybrid assay. **C:** The reduction of keratinocyte growth factor (KGF) mRNA levels in WPMY-1 cells (**top panel**) and PSA levels in LNCaP cells (**bottom panel**) after 5-μmol/L ASC-J9 treatments. **D:** ASC-J9, 5 μmol/L, treatment reduced $(ARE)_4$-luciferase (Luc) activity in WPMY-1 (**top panel**) and LNCaP cells (**bottom panel**) after DHT stimulation. **E−G:** ASC-J9 suppressed ARA70-mediated AR transcriptional activity in COS-1 cells after HF, bicalutamide, or 17β-estradiol (E2) treatment using MMTV-Luc reporter assay. ARA70 full-length (ARA70F), ARA70 N-terminal amino acid 1-401 (ARA70N), and mutant AR (T877A AR) are shown. Error bars = mean ± SD. RLA, relative luciferase activity.

ASC-J9 Promotes the Degradation of AR Protein

The initial goal was to identify a novel anti-AR compound(s) via screening natural products and their derivatives that could interrupt the interactions between AR and its selective AR coregulators in prostate stromal and luminal epithelial cells. Dissociation of the AR-coregulator complex could then result in the suppression of AR transcriptional activity. We found that AR, after being dissociated from selective coregulators, such as ARA55 or ARA70, became more susceptible to be degraded. Results from Western blot analysis showed that AR proteins in LAPC4 (wild-type AR) and LNCaP (mutant T877A AR) cells were substantially reduced after the addition of ASC-J9 in a dose-dependent manner (Figure 2A). These results were unequivocally observed in other castration-resistant PCa cell lines (C4-2 and CWR22Rv1) (Figure 2B). ASC-J9, but not the currently used or newly developed antiandrogens (bicalutamide, HF, or enzalutamide) (see Supplemental Figure S2 for each compound's structure), could promote the degradation of full-length AR in the LAPC4, LNCaP, C4-2, and CWR22Rv1 cells as well as the splice variant AR3 in the CWR22Rv1 cells (Figure 2, A and B, and Supplemental Figure S3).

The enhanced AR ubiquitination after ASC-J9 treatment seems to be one of the key mechanisms to promote AR protein degradation (Supplemental Figure S4). In contrast, AR mRNA did not show marked changes after ASC-J9 treatment in the CWR22Rv1,[20] LNCaP, and C4-2 cells (K.-P.L., unpublished data). We also assayed the ASC-J9 degradation efficiency on other nuclear receptors in various cells, including LNCaP, PC-3, and T47D cells, because some endogenous nuclear receptors are expressed only in certain types of cells. We found that ASC-J9 had a better degradation capacity on AR (LNCaP) than on other nuclear receptors, such as GR (PC-3), PPAR-α (PC-3), PPAR-γ (PC-3), RARα (LNCaP), ERα (T47D), and ERβ (T47D) (Figure 2C). As different cells have differential expression of nuclear receptors with their various associated coregulators under various concentrations of their agonists/antagonists, we might expect to see the variant degradation capacity of individual nuclear receptors with ASC-J9 treatment. A comprehensive *in vivo* toxicity study in the future may provide a better answer whether ASC-J9 may have any severe adverse effects due to targeting other proteins, including various nuclear receptors.

To dissect the molecular mechanisms by which ASC-J9 degrades AR, we tested whether ASC-J9 could influence protease degradation pathways by examining AR-Mdm2 complex formation. We found that ASC-J9 could increase the interaction of AR-Mdm2 complex in LNCaP cells

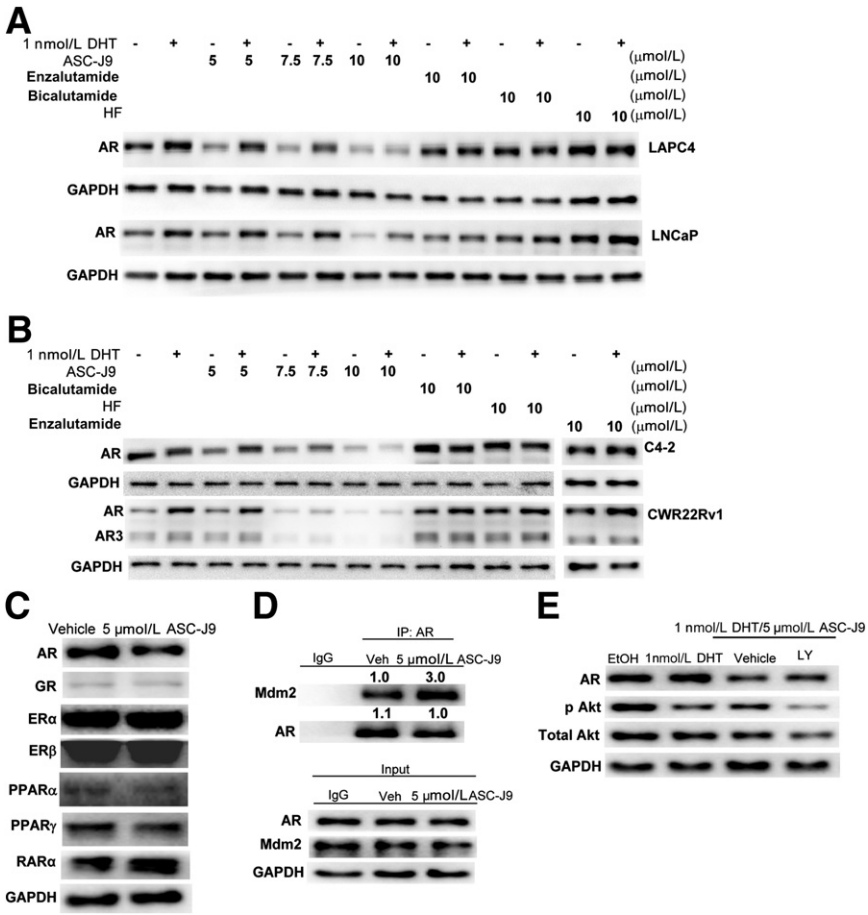

Figure 2 ASC-J9 enhances AR protein degradation through the proteasome-dependent pathway. **A:** ASC-J9, but not enzalutamide, bicalutamide, or HF, could enhance the degradation of AR proteins in LAPC4 cells and LNCaP cells using Western blot analysis. **B:** ASC-J9 degraded AR protein in castration-resistant C4-2 cells and CWR22Rv1 cells. The full blots of the enzalutamide-treated group are provided in Supplemental Figure S3. **C:** ASC-J9 had a higher degradation capacity on AR protein compared with effects on GR, ERα, ERβ, PPARα, PPARγ, and RARα Western blot analysis. The protein amounts of AR, GR, ERα, ERβ, PPARα, PPARγ, and RARα in response to 5 μmol/L ASC-J9 was determined in LNCaP cells (AR and RARα), PC3 cells (GR, PPARα, and PPARγ), and T47D breast cancer cells (ERα and ERβ). The GAPDH loading control is shown for the LNCaP cells, and GAPDH amounts in the vehicle-treated or ASC-J9—treated group were also similar in PC-3 and T47D cells (data not shown). **D:** The interaction between AR and Mdm2 was increased in MG-132 pre-treated LNCaP cells, after 5-μmol/L ASC-J9 treatments using Co-IP followed by immunoblotting assay. The quantitation data of Co-IP are presented as fold increase compared with the vehicle (Veh) group. **E:** The AR protein degradation mediated by 5 μmol/L ASC-J9 in LNCaP cells was partially reversed by treating with 5 μmol/L LY294002 (LY) 30 minutes before ASC-J9 treatment. Western blot analysis was used to characterize AR, pAkt (S473), total Akt, and GAPDH protein amounts. EtOH, ethanol.

(Figure 2D) and the phosphorylations of Akt and Mdm2, which are the key molecules involved in the proteasome-dependent pathways in C4-2 and CWR22Rv1 cells (Supplemental Figure S5). Supportively, co-treatment of ASC-J9 with the inhibitor of the PI3K/Akt (LY294002) could partially reverse AR degradation (Figure 2E). These results were further confirmed by reintroducing dominant-negative Akt (dAkt, K179M, S473A, T308A) and/or mutant Mdm2 (S166/186A) into the CWR22Rv1 cells to partially reverse ASC-J9–mediated AR degradation (Supplemental Figure S6), suggesting that ASC-J9 might promote AR degradation via the proteasome degradation pathway.[21]

Collectively, we conclude that ASC-J9 can enhance the association of AR-Mdm2, and, therefore, AR becomes more susceptible to be degraded by proteasomes (after dissociation of selective ARA interactions).

ASC-J9 Suppresses AR Transcriptional Activity through Protein Degradation

The consequences of such dissociation between AR and its selective AR coregulators via ASC-J9 might also lead to the decreased binding of androgens to AR. For relative ligand binding assays, aliquots of LNCaP cell lysates with synthetic androgen–[^{3}H] R1881 were incubated with increasing concentrations of unlabeled DHT, HF, and ASC-J9, and results showed that ASC-J9 was able to interfere with the androgen binding (Supplemental Table S1).

ASC-J9 also disrupted the AR amino- and carboxyl-terminal (N-C) interaction that is important in mediating AR transactivation.[22] As shown in Figure 3A, DHT could promote AR N-C interaction, and the addition of ASC-J9 was able to block the AR N-C interaction.

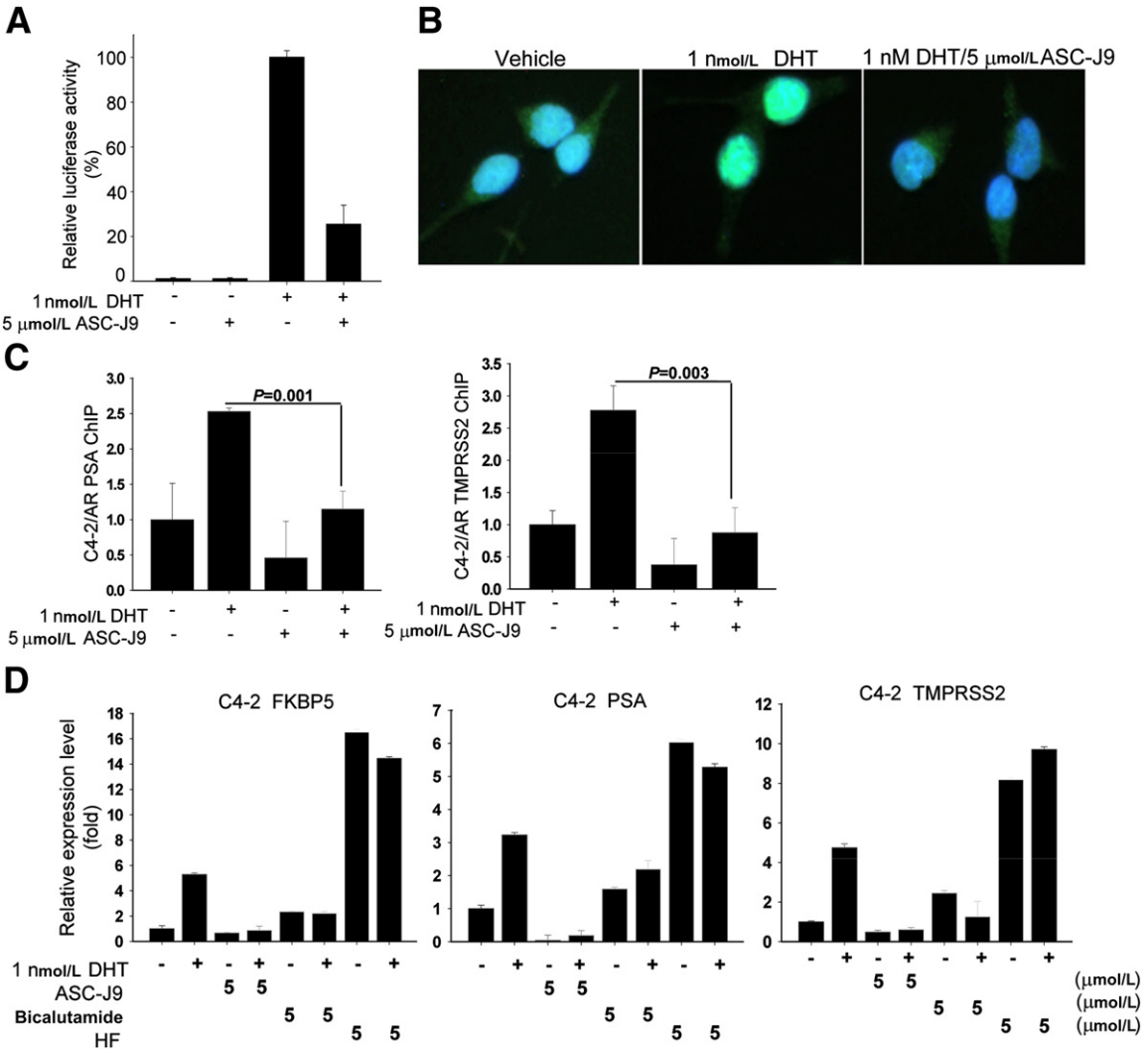

Figure 3 ASC-J9 abolishes androgen/AR signal pathways. **A:** ASC-J9 interrupted the AR N-C terminal interaction using the mammalian two-hybrid assay and the dual luciferase systems. **B:** ASC-J9 blocked AR nuclear translocation stimulated by DHT in LNCaP cells. Immunofluorescent staining was performed to determine AR localization. Green indicates AR protein and blue labels DAPI nuclear staining. **C:** ASC-J9 suppressed DHT-induced AR recruitment to *PSA* and *TMPRSS2* promoter regions in C4-2 cells using chromatin immunoprecipitation assay. The quantitative PCR results are shown from the amplification of immunoprecipitated *PSA* and *TMPRSS2* promoter regions. **D:** ASC-J9 displayed better suppressive effects on AR-targeted genes *FKBP5*, *PSA*, and *TMPRSS2* than bicalutamide and HF in C4-2 cells. The gene expression levels were determined using quantitative PCR analysis and normalized with GAPDH. Error bars = mean ± SD.

Furthermore, the DHT-induced AR nuclear translocation was blocked by co-treatment with ASC-J9 (Figure 3B). Chromatin immunoprecipitation binding assays demonstrated that ASC-J9 inhibited the recruitment of AR protein to its targeted genes (*PSA* and *TMPRSS2*) promoter regions (Figure 3C).

The consequences of the interrupted intracellular AR signals/shuttle by ASC-J9 might then result in better inhibition of AR-targeted gene expression (*FKBP5*, *PSA*, and *TMPRSS2*) than the currently used antiandrogens (bicalutamide and HF) in C4-2 cells (Figure 3D) and C81 (Supplemental Figure S7). In contrast, HF is a strong agonist for mutant AR in LNCaP, C4-2, and C81 cells.

Together, results from Figure 3 demonstrate that AR could be more easily degraded by ASC-J9 through dissociation of AR and selective AR coregulators. The AR degradation by ASC-J9, therefore, interfered with androgen/AR binding, AR N-C interaction, AR nuclear translocation, and AR recruitment to the targeted gene promoter region, which might then suppress AR transactivation and its targeted gene expressions.

ASC-J9 Inhibits PCa Cell Growth in C4-2, C81, CWR22Rv1, and LNCaP Cells

To determine the consequences of AR degradation mediated by ASC-J9, we tested the growth of AR-positive PCa cells. We first examined castration-resistant C4-2, C81, and CWR22Rv1 cells[23–25] and found that ASC-J9 significantly inhibited cell growth in these three types of cells in the presence of 1 nmol/L DHT (human prostate DHT concentration after ADT) (Figure 4A)[26,27] or 10 nmol/L DHT (human prostate DHT concentration before ADT) (Figure 4B) with better efficacy than the currently used antiandrogens, such as bicalutamide and HF (Figure 4).[28–30]

We also examined ASC-J9 effects on LNCaP cells that represent androgen-sensitive PCa before ADT.[25,31,32] We confirmed that ASC-J9 significantly inhibited cell growth of LNCaP cells in the presence of 1 or 10 nmol/L DHT (Figure 4, A and B). Collectively, the results from Figure 4 demonstrate that ASC-J9 could effectively suppress cell growth of the androgen-sensitive and castration-resistant PCa cells.

ASC-J9 Suppresses Tumor Growth of C81, C4-2, and CWR22Rv1 Cells Xenografted into Castrated Nude Mice

To demonstrate ASC-J9 *in vivo* effects, we then applied *in vivo* xenografts in castrated mouse models, which were recently used to characterize the therapeutic effects of the newly developed antiandrogens (RD162 and enzalutamide).[6] We orthotopically injected the castration-resistant PCa cells (C81, C4-2, and CWR22Rv1) into the castrated nude mice that have nearly undetectable serum testosterone[33] and observed that the xenografted C81, C4-2, and CWR22Rv1 cells were able to grow, indicating that the castration-resistant PCa could not be eliminated even after removal of almost all endogenous androgens. In contrast, i.p. injection of ASC-J9 (75 mg/kg of body

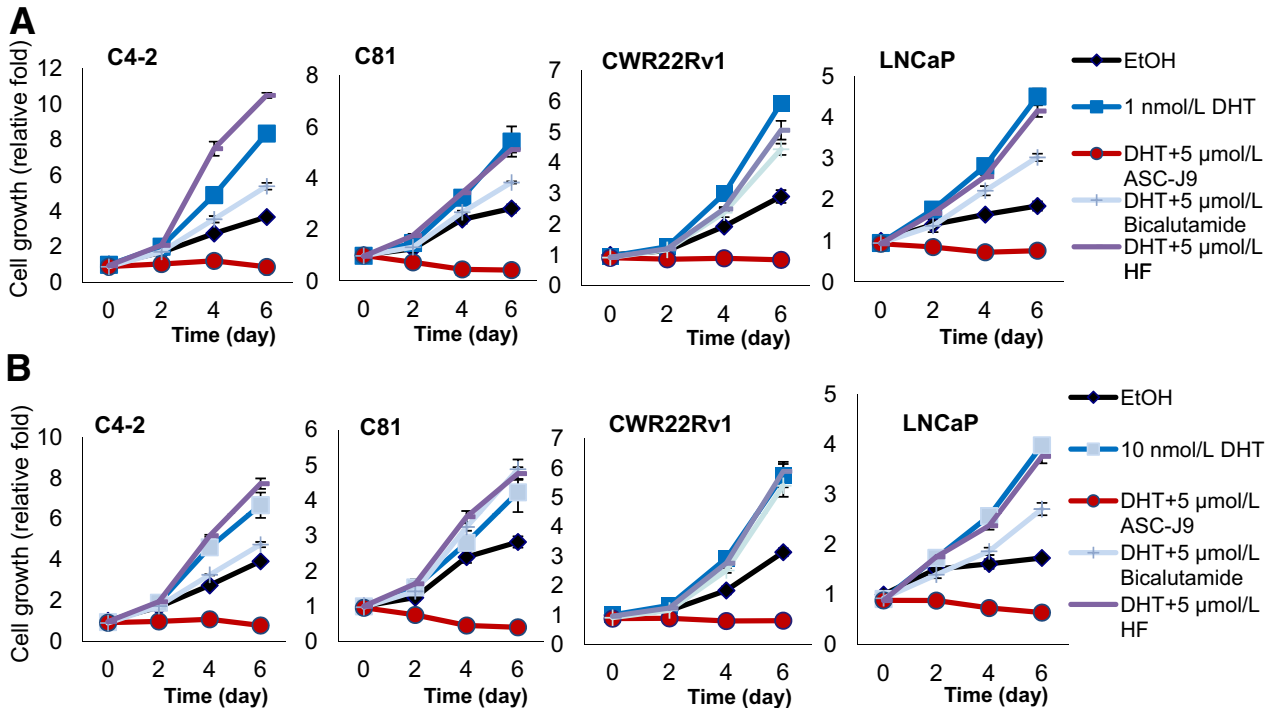

Figure 4 ASC-J9 inhibits cell growth in androgen-sensitive and castration-resistant PCa cells. ASC-J9, 5 μmol/L, treatment substantially inhibited cell growth in castration-resistant C4-2, C81, and CWR22Rv1 cells and androgen-sensitive LNCaP cells in the presence of 1 nmol/L DHT using the MTT assay (**A**) and under the 10 nmol/L DHT condition (**B**). All cell growth studies were monitored using the MTT assay and confirmed by the cell counting method. EtOH, ethanol.

weight every other day) could significantly suppress the C81 xenografted tumor growth compared with the vehicle control–treated group (Figure 5A). Similar results were obtained when we replaced C81 cells with C4-2 cells (Figure 5B) or CWR22Rv1 cells (Figure 5C). The histologic results of H&E, AR, Ki-67, and TUNEL staining in C81, C4-2, and CWR22Rv1 xenografted tumors were also examined to show ASC-J9 effects (Supplemental Figures S8 and S9). Together, these results showed that ASC-J9 could effectively degrade AR *in vivo*, resulting in suppressed cell proliferation and enhanced apoptosis in xenografted tumors.

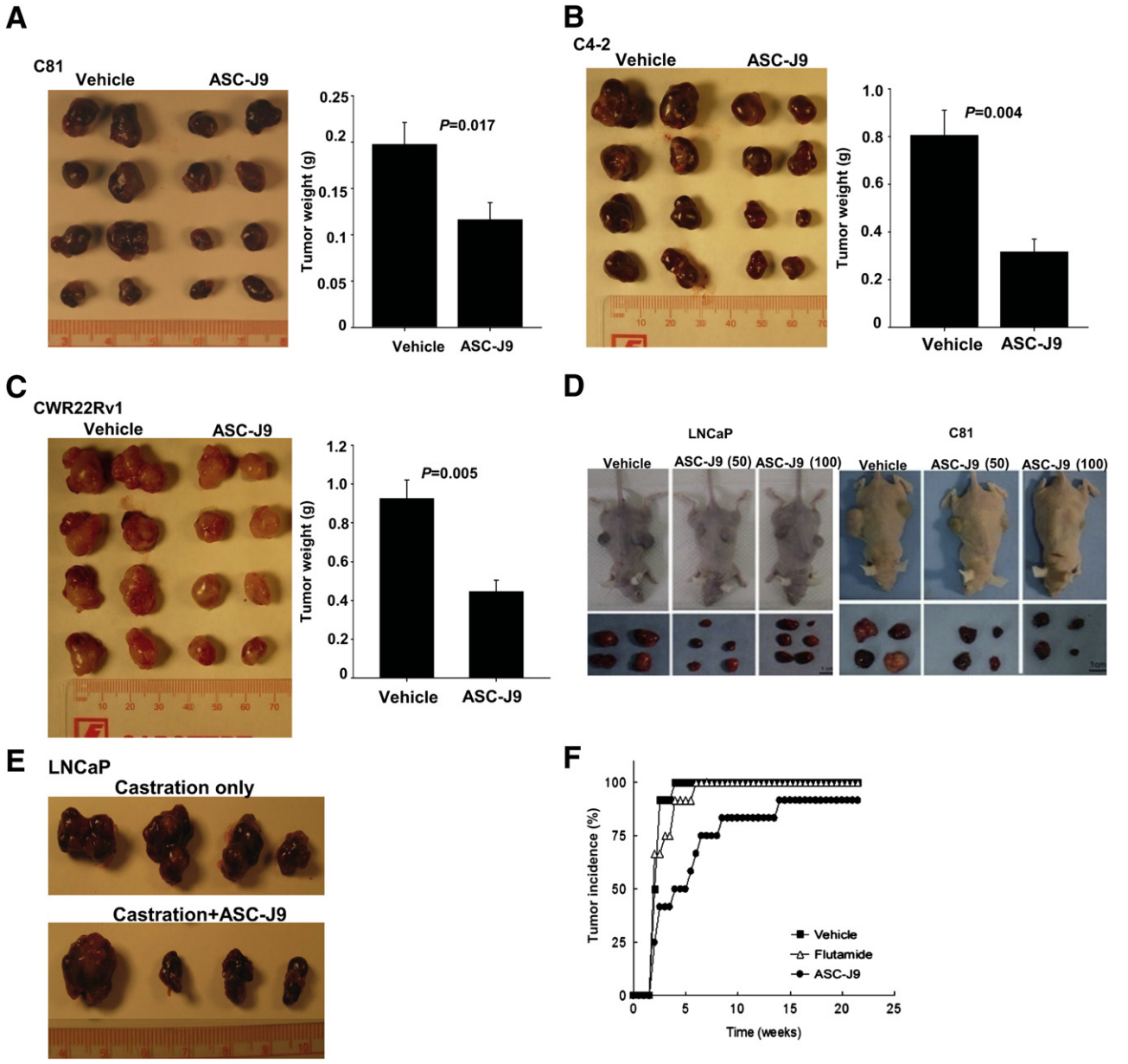

Figure 5 The *in vivo* antitumor and chemopreventive effects of ASC-J9 in the xenograft mouse PCa model. **A**: ASC-J9 suppressed C81 xenografted tumor growth in castrated nude mice. C81 cells were orthotopically implanted into anterior prostates of castrated nude mice and grown for 3 to 4 weeks. Mice were then treated with vehicle or 75 mg/kg of ASC-J9 every other day. The tumors were harvested after 3 weeks of treatment. The representative gross appearances of eight tumors from five to six mice per group (**left panel**) and the quantitation data of tumor weights (**right panel**) are shown. **B**: ASC-J9 inhibited tumor growth of C4-2 xenograft in castrated nude mice. **C**: ASC-J9 inhibited CWR22Rv1 xenografted tumor growth in castrated nude mice. **D**: ASC-J9 suppressed androgen-sensitive LNCaP (**left panel**) and androgen-insensitive C81 (**right panel**) xenografted tumor growth in intact nude mice. The 50 or 100 mg/kg of ASC-J9 was administered twice per week starting 2 to 3 weeks after s.c. implantation. The gross appearance of LNCaP and C81 xenografted nude mice (**top panels**) and the dissected prostate tumors (**bottom panels**) are shown. Scale bars: 200 μm (original magnification, ×100) and 50 μm (original magnification, ×400) **E**: ASC-J9 suppressed castration-resistant LNCaP xenografted tumor growth *in vivo*. LNCaP cells were orthotopically implanted into anterior prostates of intact nude mice and were grown for 25 to 28 days. Mice were then castrated, and ASC-J9 treatment was started 5 days after castration. The tumors were harvested after 2 weeks of treatment. $N = 4$ mice per group. **F**: ASC-J9 treatment shows significant delayed tumor incidence compared with the vehicle- and flutamide-treated groups. The ASC-J9 was injected or a flutamide pellet was implanted into 4-week-old nude mice when LNCaP cells were s.c. injected into the flanks. The palpable tumor formation was checked weekly.

ASC-J9 Inhibits LNCaP/C81 Xenografted Tumor Growth in Intact Nude Mice

We further confirmed ASC-J9 therapeutic effects in a second mouse model using LNCaP and C81 cells xenografted into nude mice without castration (to mimic human PCa development before ADT), and the results consistently showed that the i.p. injection of low-dose (50 mg/kg) or high-dose (100 mg/kg) ASC-J9 in mice showed significant inhibition of tumor growth compared with vehicle control mice (Figure 5D and Supplemental Figure S10), with little influence on their body weights (Supplemental Figure S10B).

We subsequently applied a third *in vivo* mouse model with xenografted LNCaP cells in intact mice and then castrated these nude mice after 1 month of tumor growth to examine PCa progression before and after castration. We found that the castration-resistant LNCaP xenografted tumors remained sizeable after castration treatment (Figure 5E). In contrast, ASC-J9 could further inhibit xenografted tumor growth after castration compared with the mice receiving castration only (Figure 5E). The histologic characterizations were shown and demonstrated that ASC-J9 inhibited cell proliferation and increased apoptosis through AR degradation *in vivo* (Supplemental Figure S9, B and D).

If we injected ASC-J9 at the time point when we started to xenograft LNCaP cells, we found that ASC-J9, but not HF flutamide, could also delay the xenografted tumor development (Figure 5F).

Taken together, the evidence from three different mouse models suggest that ASC-J9 could suppress the growth of prostate tumors with treatment starting at i) the castration-resistant stage after ADT (Figure 5, A–C), ii) the stage being transitioned from before to after ADT (Figure 5, D and E), and iii) initial PCa growth stage (Figure 5F).

Therapeutic and Chemopreventive Effects of ASC-J9 in Spontaneous PCa Development TRAMP Mouse Models

There are few perfect PCa mouse models that can mimic human PCa development/progression. Therefore, we decided to use the two currently available spontaneous PCa development mouse models (transgenic adenocarcinoma of the mouse prostate, TRAMP, and phosphatase and tensin homolog, *Pten*$^{+/-}$) to further confirm the ASC-J9 *in vivo* effect, as we believe that the xenografted mouse models might have limitations when attempting to mimic the physiologic condition of the prostate microenvironment.

We performed i.p. injection of 75 mg/kg of ASC-J9 daily into 8-week-old C57BL/6/FVB TRAMP mice[34] (that have already developed precancerous lesions) for 4 months, and results showed that ASC-J9 could suppress tumor development (Figure 6A). The body weights of the ASC-J9–injected mice were comparable with the vehicle-treated mice (Supplemental Figure S11A). Moreover, H&E staining and SV40-Tag immunohistochemical staining were concurrently examined (Supplemental Figure S11B) to demonstrate that ASC-J9 could effectively suppress PCa progression. In addition, we also performed AR immunohistochemical staining, BrdU staining for proliferation assay, and the TUNEL apoptosis assay to characterize PCa tumor growth between the vehicle- and ASC-J9–treated groups. The results indicate that ASC-J9 was able to decrease AR protein levels, reduce proliferation, and increase apoptosis (Supplemental Figure S11, C and D).

We then applied another approach using 33- to 34-week-old TRAMP mouse prostate tumor chunks (cut into 0.2-cm tissue chunks), s.c. implanted into SCID mice to confirm the ASC-J9 *in vivo* effect. After 2 weeks of implantation, vehicle or ASC-J9 was injected every other day for 4 weeks before harvest. The results consistently showed that subcutaneous tumor size/weight was significantly reduced in the ASC-J9–treated mice (Figure 6B). H&E staining of the subcutaneous TRAMP tumors and assays of AR protein, BrdU, and TUNEL were examined (Supplemental Figure S12, A-C). The results demonstrate that ASC-J9 could effectively degrade AR *in vivo*, leading to the inhibition of TRAMP tumor growth.

We further confirmed this finding by implanting TRAMP mouse prostate tumor chunks into the renal capsule of SCID mice to validate the ASC-J9 effects, and we obtained results similar to those for the s.c. implanted tumors (Figure 6C).

It has been known that the expression of SV40-Tag in TRAMP mice is driven by the probasin promoter, in which androgen/AR plays a crucial regulatory role. The previous report has documented that castration in TRAMP mice could cause some tumor regression; however, some of the tumors still continue to grow, indicating the heterogeneity of the primary tumor, and the overall progression to poorly differentiated and metastatic tumor was not ultimately delayed after castration.[35] Further analysis of AR and SV40-Tag after castration found that the AR level was significantly elevated, but SV40-Tag expression almost disappeared 10 weeks after castration.[35] Critically, 20 weeks after castration, the expression level of SV40-Tag was comparable with that of intact mice, suggesting that probasin promoter still could function normally 20 weeks after castration; therefore, other transcriptional machinery might be able to account for the promoter activation under castration.[35] Overall, castration could initially inhibit SV40-Tag expression through the suppression of androgen/AR signals; however, 20 weeks after castration, the SV40-Tag level was relatively comparable.[36] In this regard, we observed that ASC-J9 suppressed TRAMP mouse tumor progression was not due to early inhibition of SV40-Tag transgene expression alone. More importantly, the suppression of AR-mediated tumor growth might be one of the reasons that ASC-J9 could suppress PCa development in TRAMP mice.

Chemopreventive Effects of ASC-J9 in *Pten*$^{+/-}$ Mouse Models

Next, we applied the second mouse model (*Pten*$^{+/-}$ mouse) that could spontaneously develop precancerous lesions to

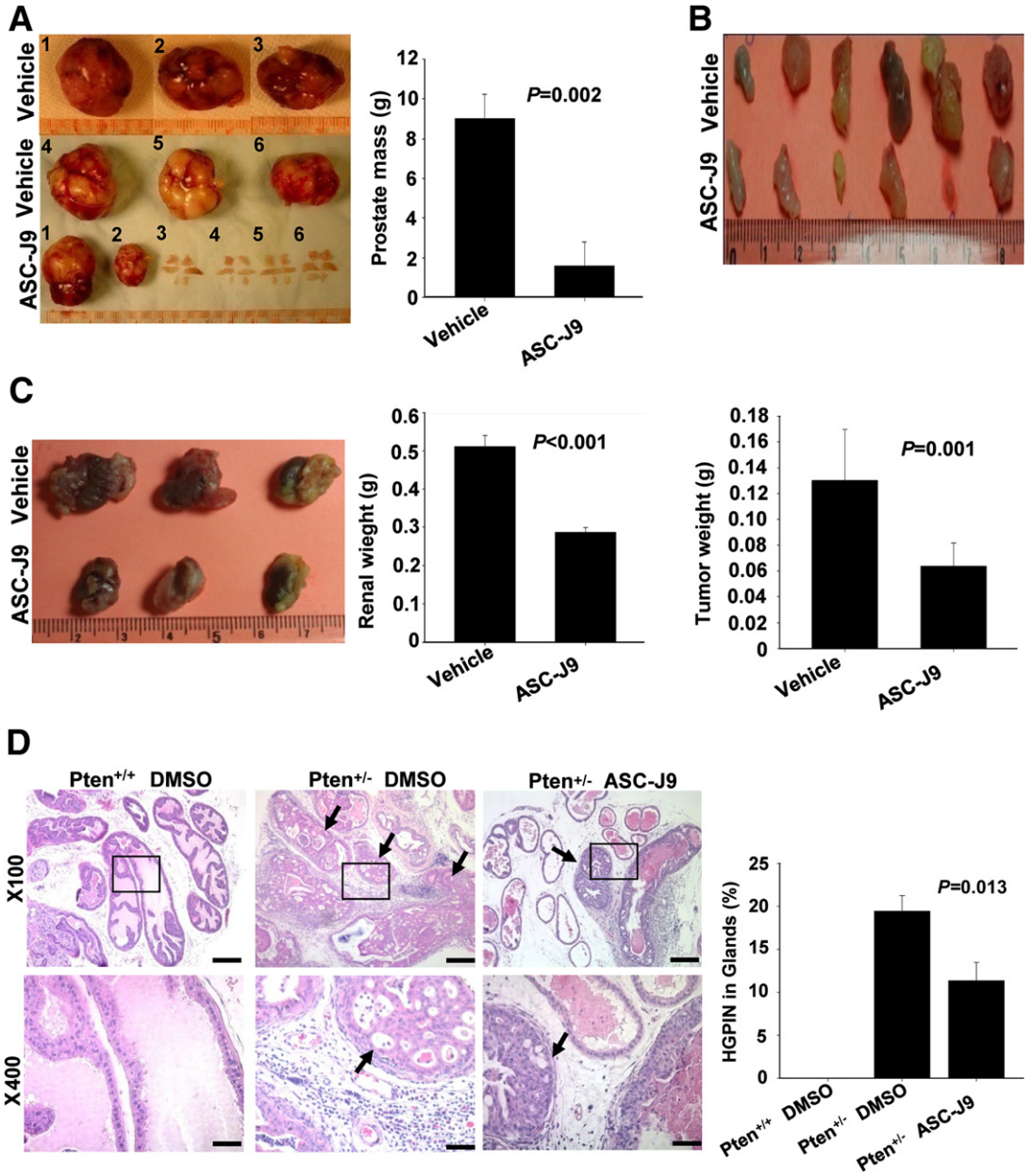

Figure 6 *In vivo* therapeutic and chemopreventive effects of ASC-J9 in genetically engineered mouse PCa models. **A**: Early treatment with ASC-J9 suppressed tumor initiation/progression in the TRAMP mouse model. The chemopreventive effects of ASC-J9 were demonstrated by early i.p. injection at 8 weeks old with continued treatment until 23 to 24 weeks old. The prostates (prostate tumors or precancerous lesions) were harvested and photographed (**left panel**), and the prostate mass weights were calculated (**right panel**). $N = 6$ mice per group. **B**: ASC-J9 treatment suppressed the growth of TRAMP tumor chunks s.c. implanted into SCID mice. After 4 weeks of vehicle or ASC-J9 injection, the s.c. tumors were harvested and photographed (**top panel**), and the tumor weights were calculated (**bottom panel**). $N = 6$ for each group. **C**: TRAMP prostate tumor growth was inhibited by ASC-J9 after subrenal capsule implantation in SCID mice. After 4 weeks of vehicle or ASC-J9 injection, tumors were harvested and photographed (**left panel**), and the tumor weights were determined (**right panel**). $N = 3$ for each group. **D**: ASC-J9 displayed chemopreventive effects in the *Pten*$^{+/-}$ mouse model. ASC-J9 was administrated to 6-month-old *Pten*$^{+/-}$ mice, and the dorsolateral prostates were harvested 2 months after injection. Histologic examination of 8-month-old *Pten*$^{+/+}$ DMSO, *Pten*$^{+/-}$ DMSO, and *Pten*$^{+/-}$ ASC-J9—treated prostates were subjected to H&E staining (**left panel**). The **arrows** point to the high-grade PIN lesions. Quantitation of high-grade PIN lesions is provided in the **right panel**. $N = 5$ to 6 mice per group. Error bars = mean ± SEM. Scale bars: 200 μm (original magnification, ×100) and 50μm (original magnifcation, ×400).

confirm the ASC-J9 effect. Unlike TRAMP mice, *Pten*$^{+/-}$ mice developed only low-/high-grade prostatic intraepithelial neoplasia (PIN) lesions.[12] Early reports (in humans) indicated that approximately 5% to 10% of high-grade PIN could be detected via the needle prostate biopsy,[37] and it is considered as an early stage of PCa,[38] with a 50% to 75% high risk of subsequent PCa development.[39] To prove the ASC-J9 effects, we started injection of either vehicle or ASC-J9 into 6-month-old *Pten*$^{+/-}$ mice every other day for 2 months and harvested the prostate tissues for histologic characterization. We observed that the dorsolateral prostates from ASC-J9-injected *Pten*$^{+/-}$ mice

showed diminished high-grade PIN formation, and the quantitation data are provided (Figure 6D).

Together, results from the previously mentioned two mouse models (TRAMP and *Pten*$^{+/-}$) confirm the previous xenografted tumor results (Figure 5) and demonstrate that ASC-J9 treatment represents a more effective antitumor therapy compared with the currently used surgical or medical castration. More important, ASC-J9 might represent the first anti-AR compound that could further suppress tumor growth after ADT in the castration-resistant stage.

Few Adverse Effects and Little Toxicity in Mice Treated with ASC-J9

During the *in vivo* mouse studies, as described in Figures 5 and 6, we observed that the mice receiving ASC-J9 (50 to 100 mg/kg of body weight) showed few adverse effects. Their body weights were similar to those of the control mice (Supplemental Figures S10B and S11A). More importantly, we observed that the ASC-J9–treated mice had normal serum testosterone levels with normal sexual activity (judged by vaginal plug numbers in female mice caged with the treated males[14]), suggesting that there was little adverse influence on serum testosterone in the sexual functions in the ASC-J9–treated mice. This is important for improvement of the quality of life for patients with PCa receiving the current ADT with adverse effects of low serum testosterone concentrations and decreased libido.[40]

Moreover, using ASC-J9 as an AR degradation enhancer to treat acne vulgaris, AndroScience Corp. has completed phase 1 studies (in healthy individuals and patients with acne, separately) and phase 2 trial (in patients with acne), and results showed few adverse effects in these trials.

Discussion

The initial screening strategy to identify ASC-J9 was based on interruption of the AR-ARA55 and/or AR-ARA70 complex that exists mainly in either prostate stromal or luminal epithelial cells, in which AR functions as positive roles to promote PCa progression. We found that the mice receiving ASC-J9 had normal body weight with normal serum testosterone levels and sexual activity with few adverse effects, suggesting that ASC-J9 could be different from the current antiandrogens, such as HF, bicalutamide, and enzalutamide, which reduce/prevent androgens from binding to the AR in the whole body and cause adverse effects, including decreased libido. Because stromal cells and luminal epithelial cells exist in most stages of PCa, including before and after ADT (Supplemental Figure S13), and continue to promote PCa progression,[3,4,41] we believe that targeting AR in selective cells via ASC-J9 might represent a better strategy for battling PCa.

More importantly, this strategy could be applicable to inhibiting tumor growth in the castration-resistant stage (see results in mice under castration conditions that have nearly undetectable serum androgen levels in Figure 5, A–C and E, and human PCa cells at the ADT condition of 1 nmol/L DHT in Figure 4A), showing that ASC-J9, but not the surgical or chemical castration, could further suppress PCa growth, suggesting that targeting AR protein degradation instead of targeting androgens may represent a new and better strategy for battling PCa in the castration-resistant stage.

Molecular mechanism dissection suggested the following conclusions. First, ASC-J9 might interrupt the interaction between AR and selective coregulators that leads to promotion of AR degradation via the proteasome degradation pathway. The activation of Akt and Mdm2 by ASC-J9 treatment could subsequently trigger AR ubiquitination, resulting in AR degradation. Second, ASC-J9–mediated AR degradation might consequently abolish androgen-AR binding, AR N-C interaction, AR nuclear translocation, and AR recruitment to targeted gene promoter regions, leading to the inhibition of AR transcriptional activity. Third, ASC-J9–mediated AR degradation might thereby suppress PCa progression through the alteration of multiple signal pathways. Using gene array and subsequent real-time-PCR analyses to examine genes related to PCa progression,[42,43] we found that ASC-J9–treated LNCaP/C81 xenografted tumors had reduced expression of angiogenesis and metastasis-related genes, such as *bFGF*, *VEGF*, and *MMP9* (Supplemental Figure S14A). Moreover, ASC-J9 also modulated the toll-like receptor 3 pathway and its downstream caspase gene expressions (*Caspase 3, 8, 9*), as well as the proapoptotic protein (BAX), and apoptosis-inducing factor in LNCaP cells (Supplemental Figure S14B). This was further confirmed in the ASC-J9–treated TRAMP mouse tumors by showing elevated levels of several apoptosis-related genes, such as tumor necrosis factor (*TNF*), caspase-8 (*Casp8*), CASP8 and FADD-like apoptosis regulator (*Cflar*), and telomerase reverse transcriptase (*Tert*) (Supplemental Figure S14C and Supplemental Table S2). The gene array data from multiple ASC-J9–treated tumors led us to conclude that interference of androgen/AR signals by ASC-J9 might, therefore, modulate multiple signal pathways to suppress PCa growth/progression.

Removal of androgen by ADT causes PCa cell apoptosis,[44] yet tumors may still develop castration resistance even at 1 to 3 nmol/L minimal castrated level of androgens.[45] Indeed, more evidence indicates that castration-resistant prostate tumors still maintain relatively higher AR amounts via either AR gene amplification or other mechanisms.[46] The current ADT with available antiandrogens, such as bicalutamide, HF, and enzalutamide (that showed better efficacy to inhibit androgen binding to AR), all failed to target and degrade the remaining AR in prostate tumors at the castration-resistant stage.[6] Similarly, the azole antifungal agent ketoconazole[47] or abiraterone acetate,[48] which could suppress the biosynthesis of adrenal androgens, also failed to ablate the remaining AR; although clinical trials had shown that these compounds could increase median survival with decreased PSA levels in patients.[49]

Early studies suggested that the AR splice variants might contribute to the progression of PCa into castration resistance, especially the most dominant variant AR-V7/AR3, which lacks the portion of the androgen-binding domain; whereas, the current antiandrogens failed to suppress AR3-mediated transcriptional activity.[50] It has been suggested that the constitutively active AR3 relies on full-length AR to exert the AR transcriptional activity and cell growth in LNCaP-AR cells.[51] However, another study also demonstrated that AR3 itself might contribute to promoting cell growth.[50] Therefore, it would be better to target full-length AR and AR3 to achieve superior therapeutic efficacy in castration-resistant PCa. In a previous report[20] and the present study (Figure 2B), we showed that ASC-J9 could degrade full-length AR and AR3 in CWR22Rv1 cells.

In summary, this study characterizes the first AR degradation enhancer, ASC-J9, which is different from the currently used antiandrogens that could selectively degrade AR protein to suppress AR signaling and tumor growth *in vitro* and *in vivo*. The success of tumor regression with ASC-J9 in androgen-dependent and castration-resistant PCa may provide a new and more effective therapeutic approach for battling PCa in future.

Acknowledgment

We thank Karen Wolf (George H. Whipple Laboratory for Cancer Research, University of Rochester, Rochester, NY) for assistance in manuscript preparation.

Supplemental Data

Supplemental material for this article can be found at *http://dx.doi.org/10.1016/j.ajpath.2012.10.029*.

References

1. Chen CD, Welsbie DS, Tran C, Baek SH, Chen R, Vessella R, Rosenfeld MG, Sawyers CL: Molecular determinants of resistance to antiandrogen therapy. Nat Med 2004, 10:33−39
2. Heinlein CA, Chang C: Androgen receptor in prostate cancer. Endocr Rev 2004, 25:276−308
3. Niu Y, Altuwaijri S, Lai KP, Wu CT, Ricke WA, Messing EM, Yao J, Yeh S, Chang C: Androgen receptor is a tumor suppressor and proliferator in prostate cancer. Proc Natl Acad Sci U S A 2008, 105: 12182−12187
4. Niu Y, Altuwaijri S, Yeh S, Lai KP, Yu S, Chuang KH, Huang SP, Lardy H, Chang C: Targeting the stromal androgen receptor in primary prostate tumors at earlier stages. Proc Natl Acad Sci U S A 2008, 105: 12188−12193
5. Lilja H, Ulmert D, Vickers AJ: Prostate-specific antigen and prostate cancer: prediction, detection and monitoring. Nat Rev Cancer 2008, 8: 268−278
6. Tran C, Ouk S, Clegg NJ, Chen Y, Watson PA, Arora V, Wongvipat J, Smith-Jones PM, Yoo D, Kwon A, Wasielewska T, Welsbie D, Chen CD, Higano CS, Beer TM, Hung DT, Scher HI, Jung ME, Sawyers CL: Development of a second-generation antiandrogen for treatment of advanced prostate cancer. Science 2009, 324:787−790
7. Niu Y, Chang TM, Yeh S, Ma WL, Wang YZ, Chang C: Differential androgen receptor signals in different cells explain why androgen-deprivation therapy of prostate cancer fails. Oncogene 2010, 29: 3593−3604
8. Wu CT, Altuwaijri S, Ricke WA, Huang SP, Yeh S, Zhang C, Niu Y, Tsai MY, Chang C: Increased prostate cell proliferation and loss of cell differentiation in mice lacking prostate epithelial androgen receptor. Proc Natl Acad Sci U S A 2007, 104:12679−12684
9. Lai KP, Yamashita S, Vitkus S, Shyr CR, Yeh S, Chang C: Suppressed prostate epithelial development with impaired branching morphogenesis in mice lacking stromal fibromuscular androgen receptor. Mol Endocrinol 2012, 26:52−66
10. Lai KP, Yamashita S, Huang CK, Yeh S, Chang C: Loss of stromal androgen receptor leads to suppressed prostate tumourigenesis via modulation of pro-inflammatory cytokines/chemokines. EMBO Mol Med 2012, 4:791−807
11. Chang CS, Kokontis J, Liao ST: Molecular cloning of human and rat complementary DNA encoding androgen receptors. Science 1988, 240:324−326
12. Podsypanina K, Ellenson LH, Nemes A, Gu J, Tamura M, Yamada KM, Cordon-Cardo C, Catoretti G, Fisher PE, Parsons R: Mutation of Pten/Mmac1 in mice causes neoplasia in multiple organ systems. Proc Natl Acad Sci U S A 1999, 96:1563−1568
13. Wu MH, Ma WL, Hsu CL, Chen YL, Ou JH, Ryan CK, Hung YC, Yeh S, Chang C: Androgen receptor promotes hepatitis B virus-induced hepatocarcinogenesis through modulation of hepatitis B virus RNA transcription. Sci Transl Med 2010, 2:32ra35
14. Yang Z, Chang YJ, Yu IC, Yeh S, Wu CC, Miyamoto H, Merry DE, Sobue G, Chen LM, Chang SS, Chang C: ASC-J9 ameliorates spinal and bulbar muscular atrophy phenotype via degradation of androgen receptor. Nat Med 2007, 13:348−353
15. Vanaja DK, Mitchell SH, Toft DO, Young CY: Effect of geldanamycin on androgen receptor function and stability. Cell Stress Chaperones 2002, 7:55−64
16. Fujimoto N, Yeh S, Kang HY, Inui S, Chang HC, Mizokami A, Chang C: Cloning and characterization of androgen receptor coactivator: ARA55, in human prostate. J Biol Chem 1999, 274: 8316−8321
17. Heinlein CA, Chang C: Androgen receptor (AR) coregulators: an overview. Endocr Rev 2002, 23:175−200
18. Fujimoto N, Mizokami A, Harada S, Matsumoto T: Different expression of androgen receptor coactivators in human prostate. Urology 2001, 58:289−294
19. Hu YC, Yeh S, Yeh SD, Sampson ER, Huang J, Li P, Hsu CL, Ting HJ, Lin HK, Wang L, Kim E, Ni J, Chang C: Functional domain and motif analyses of androgen receptor coregulator ARA70 and its differential expression in prostate cancer. J Biol Chem 2004, 279: 33438−33446
20. Yamashita S, Lai KP, Chuang KL, Xu D, Miyamoto H, Tochigi T, Pang ST, Li L, Arai Y, Kung HJ, Yeh S, Chang C: ASC-J9 suppresses castration-resistant prostate cancer growth through degradation of full-length and splice variant androgen receptors. Neoplasia 2012, 14: 74−83
21. Hoeller D, Dikic I: Targeting the ubiquitin system in cancer therapy. Nature 2009, 458:438−444
22. Hsu CL, Chen YL, Ting HJ, Lin WJ, Yang Z, Zhang Y, Wang L, Wu CT, Chang HC, Yeh S, Pimplikar SW, Chang C: Androgen receptor (AR) NH2- and COOH-terminal interactions result in the differential influences on the AR-mediated transactivation and cell growth. Mol Endocrinol 2005, 19:350−361
23. Igawa T, Lin FF, Lee MS, Karan D, Batra SK, Lin MF: Establishment and characterization of androgen-independent human prostate cancer LNCaP cell model. Prostate 2002, 50:222−235
24. Sramkoski RM, Pretlow TG II, Giaconia JM, Pretlow TP, Schwartz S, Sy MS, Marengo SR, Rhim JS, Zhang D, Jacobberger JW: A new human prostate carcinoma cell line, 22Rv1. In Vitro Cell Dev Biol Anim 1999, 35:403−409

25. Thalmann GN, Sikes RA, Wu TT, Degeorges A, Chang SM, Ozen M, Pathak S, Chung LW: LNCaP progression model of human prostate cancer: androgen-independence and osseous metastasis. Prostate 2000, 44:91−103
26. Marks LS, Mostaghel EA, Nelson PS: Prostate tissue androgens: history and current clinical relevance. Urology 2008, 72:247−254
27. Mohler JL: Castration-recurrent prostate cancer is not androgen-independent. Adv Exp Med Biol 2008, 617:223−234
28. Chodak G, Gomella L, Phung de H: Combined androgen blockade in advanced prostate cancer: looking back to move forward. Clin Genitourin Cancer 2007, 5:371−378
29. Kelly WK, Scher HI: Prostate specific antigen decline after antiandrogen withdrawal: the flutamide withdrawal syndrome. J Urol 1993, 149:607−609
30. Van Allen EM, Ryan CJ: Novel secondary hormonal therapy in advanced prostate cancer: an update. Curr Opin Urol 2009, 19: 315−321
31. Youm YH, Kim S, Bahk YY, Yoo TK: Proteomic analysis of androgen-independent growth in low and high passage human LNCaP prostatic adenocarcinoma cells. BMB Rep 2008, 41:722−727
32. Lin HK, Hu YC, Yang L, Altuwaijri S, Chen YT, Kang HY, Chang C: Suppression versus induction of androgen receptor functions by the phosphatidylinositol 3-kinase/Akt pathway in prostate cancer LNCaP cells with different passage numbers. J Biol Chem 2003, 278: 50902−50907
33. Umekita Y, Hiipakka RA, Kokontis JM, Liao S: Human prostate tumor growth in athymic mice: inhibition by androgens and stimulation by finasteride. Proc Natl Acad Sci U S A 1996, 93:11802−11807
34. Gingrich JR, Barrios RJ, Morton RA, Boyce BF, DeMayo FJ, Finegold MJ, Angelopoulou R, Rosen JM, Greenberg NM: Metastatic prostate cancer in a transgenic mouse. Cancer Res 1996, 56: 4096−4102
35. Gingrich JR, Barrios RJ, Kattan MW, Nahm HS, Finegold MJ, Greenberg NM: Androgen-independent prostate cancer progression in the TRAMP model. Cancer Res 1997, 57:4687−4691
36. Tang Y, Wang L, Goloubeva O, Khan MA, Zhang B, Hussain A: Divergent effects of castration on prostate cancer in TRAMP mice: possible implications for therapy. Clin Cancer Res 2008, 14: 2936−2943
37. Ayala AG, Ro JY: Prostatic intraepithelial neoplasia: recent advances. Arch Pathol Lab Med 2007, 131:1257−1266
38. Cheng L, Paterson RF, Beck SD, Parks J: Prostatic intraepithelial neoplasia: an update. Clin Prostate Cancer 2004, 3:26−30
39. Raviv G, Janssen T, Zlotta AR, Descamps F, Verhest A, Schulman CC: Prostatic intraepithelial neoplasia: influence of clinical and pathological data on the detection of prostate cancer. J Urol 1996, 156:1050−1054
40. Berges R, Bello U: Effect of a new leuprorelin formulation on testosterone levels in patients with advanced prostate cancer. Curr Med Res Opin 2006, 22:649−655
41. Sung SY, Chung LW: Prostate tumor-stroma interaction: molecular mechanisms and opportunities for therapeutic targeting. Differentiation 2002, 70:506−521
42. Miyamoto H, Altuwaijri S, Cai Y, Messing EM, Chang C: Inhibition of the Akt, cyclooxygenase-2, and matrix metalloproteinase-9 pathways in combination with androgen deprivation therapy: potential therapeutic approaches for prostate cancer. Mol Carcinog 2005, 44: 1−10
43. Trojan L, Thomas D, Knoll T, Grobholz R, Alken P, Michel MS: Expression of pro-angiogenic growth factors VEGF, EGF and bFGF and their topographical relation to neovascularisation in prostate cancer. Urol Res 2004, 32:97−103
44. Heidenreich A, Pfister D, Ohlmann CH, Engelmann UH: Androgen deprivation for advanced prostate cancer, [in German]. Urologe A 2008, 47:270−283
45. Mitchell RE, Chang SS: Current controversies in the treatment of high-risk prostate cancer. Curr Opin Urol 2008, 18:263−268
46. Scher HI, Sawyers CL: Biology of progressive, castration-resistant prostate cancer: directed therapies targeting the androgen-receptor signaling axis. J Clin Oncol 2005, 23:8253−8261
47. Ryan CJ, Halabi S, Ou SS, Vogelzang NJ, Kantoff P, Small EJ: Adrenal androgen levels as predictors of outcome in prostate cancer patients treated with ketoconazole plus antiandrogen withdrawal: results from a cancer and leukemia group B study. Clin Cancer Res 2007, 13:2030−2037
48. Leroux F: Inhibition of p450 17 as a new strategy for the treatment of prostate cancer. Curr Med Chem 2005, 12:1623−1629
49. Ryan CJ, Weinberg V, Rosenberg J, Fong L, Lin A, Kim J, Small EJ: Phase II study of ketoconazole plus granulocyte-macrophage colony-stimulating factor for prostate cancer: effect of extent of disease on outcome. J Urol 2007, 178:2372−2376
50. Guo Z, Yang X, Sun F, Jiang R, Linn DE, Chen H, Kong X, Melamed J, Tepper CG, Kung HJ, Brodie AM, Edwards J, Qiu Y: A novel androgen receptor splice variant is up-regulated during prostate cancer progression and promotes androgen depletion-resistant growth. Cancer Res 2009, 69:2305−2313
51. Watson PA, Chen YF, Balbas MD, Wongvipat J, Socci ND, Viale A, Kim K, Sawyers CL: Constitutively active androgen receptor splice variants expressed in castration-resistant prostate cancer require full-length androgen receptor. Proc Natl Acad Sci U S A 2010, 107:16759−16765